History of Medicine Studies
ISSN:1300-669
Volume 20 Issue 2 Sep 2024

Synthesis, DFT Analysis, and In Vitro Assessment of New Hydrazone's Cytotoxic and Cytoprotective Effects on SH-SY5YNeuroblastoma Cell Lines and Antioxidant Properties

1. **T. Vinod Kumar***, Asst. Professor, DEPT OF Pharmaceutical Analysis
2. P. Sasiklala, Asst. Professor, DEPT OF Pharmacy Practice
3. M.V. Sai Charan, Asst. Professor, DEPT OF Pharmacy Practice
4. G. R K Mohan, Asso. Professor, DEPT OF PHARMACEUTICS
5. **Dr.M.SREENIVASULU**, PRINCIPAL, NARAYANA PHARMACY COLLEGE
[1,2,3,4,5] NARAYANA PHARMACY COLLEGE, CHINTHA REDDY PALEM, NELLORE

Abstract: Ten novel hydrazide–hydrazone derivatives with a pyrrole ring were created and their structures clarified using suitable spectroscopic features. The 1,1-diphenyl-2-picrylhydrazyl (DPPH) and 2,2′-azino-bis(3-ethylbenzothiazoline-6-sulphonic acid) (ABTS) assays were used to evaluate the target hydrazones' capacity to scavenge radicals, using ethyl 5-(4-bromophenyl)Hydrozine-yl)-2-oxoethyl-1-(2-(2-(4-hydroxy-3,5-dimethoxybenzylidene))7d) ethyl 5-(4-bromophenyl) and 2-methyl-1H-pyrrole-3-carboxylateZine-yl)-3-oxopropyl hydrazine-(3-(2-(4-hydroxy-3,5-dimethoxybenzylidene))-2-methyl-1H-pyrrole-3-carboxylate (8d) was identified as the series' top radical scavenger. The best radical scavenging ligands in the newly synthesised compounds are stable, do not break down into elements, are less polarisable, and have a hard nature, according to further density functional theory (DFT) research. The compounds' significant electron donating capabilities were shown by the energy of the highest occupied molecular orbital (HOMO).All things considered, 7d and 8d may easily scavenge free radicals in biological systems by donating hydrogen atoms and transferring a single electron. The compound's protective action was evaluated in vitro using the H2O2-induced oxidative stress paradigm on the human neuroblastoma cell line SH-SY5Y. The results showed that 7das was the most representative chemical with the maximum protection and the lowest cellular damage.

Keywords: pyrrole; synthesis; DFT; antioxidant; SH-SY5Y; cellulartoxicity; cellprotection

1. Introduction

Normal biological activities are disrupted when reactive oxygen species (ROS) are generated because they cause oxidative damage to biomolecules, including cellular proteins, lipids, and DNA [1]. Oxidative stress rises as a result of a slow deterioration in cellular antioxidant defence systems brought on by the production of ROS as people age. Therefore, the development of many neurodegenerative diseases, such as Parkinson's disease (PD), Alzheimer's disease (AD), Huntington's disease (HD), amyotrophic lateral sclerosis (ALS), and many others, depends on ageing, different genetic mutations, environmental influences, and the resulting increase in oxidative stress [2].Therefore, many initiatives that provide effective neuroprotection in the treatment of neurodegenerative illnesses are based on the development of new active compounds with antioxidant potential [3].
Many commercially available medications that include pyrrolering exhibit a variety of pharmacological actions, including antipsychotics [4], antidepressants [5], anticonvulsants [6], and anti-inflammatory medicines [7].and several others. Pyrroles and pyrrole derivatives with shown antioxidant properties are gaining attention [8,9].Numerous heterocyclic hydrazones have also shown neuroprotective and antioxidant properties [10].
For instance, utilising the DPPH and ABTS techniques, Boulebd et al. [11] effectively synthesised a number of novel phenolic hydrazide-hydrazone derivatives and evaluated their capacity to scavenge radicals. Trolox, a chemical with provenantioxidant activity, and ascorbic acid were used to compare the effects.

History of Medicine Studies
ISSN:1300-669
Volume 20 Issue 2 Sep 2024

The newly synthesised compounds were shown to have antioxidant activity on par with that of Trolox and ascorbic acid [11].Another research [12] used DPPH, ABTS, and DMSO alkaline tests to assess the antioxidant activity of twelve heterocyclic compounds with hydrazone functional groups.The findings demonstrated the strong anti-radical properties of these heterocyclic compounds [12].Furthermore, using DPPH and ABTS assays, a preliminary study by Tzankova et al. [13] revealed the promising radical scavenging potential of pyrrole-based hydrazones, directing our attention towards the synthesis of analogous representatives in an effort to increase the variety of molecules. As previously detailed by Bijevetal, the first hydrazides used in the present work were synthesised in our lab.[14] for Georgiaetal and Hydrazide 7.[15] for hydrazide 8 with Figure 1 showing its overall structure.

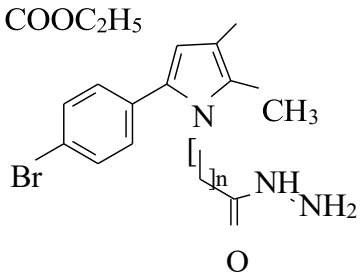

n=1(**7**)andn=2(**8**)

Figure 1. General structureoftheinitialpyrrolehydrazides.

The synthesis of novel hydrazones with a pyrrole ring system, their in vitro safety profile on human neuroblastomaSH-SY5Y cells, their radical scavenging activity using 1,1-diphenyl-2-picrylhydrazyl (DPPH) and 2,2′-azino-bis(3-ethylbenzothiazoline-6-sulphonic acid) (ABTS) assays, and an in silico evaluation of potential antioxidant mechanisms using DFT calculations are the main objectives of the following study.In a model of oxidative stress caused by H2O2 on SH-SY5Y cells, the antioxidative protective qualities of the most promising structures are assessed.

2. Results

Chemistry

The N-pyrrolyl hydrazide synthesis 8 (ethyl 5-(4-bromophenyl)-1-(3-hydrazinyl-3-oxopropyl) and 7 (ethyl 5-(4-bromophenyl)-1-(2-hydrazinyl-2-oxoethyl)-2-methyl-1H-pyrrole-3-carboxylate)1-H-pyrrole-3-carboxylate-2-methyl A Pal-Kotrcyclization reaction based on the C-alkylation of a 1,3-dicarbonyl compound to the corresponding 1,4-dicarbonyl derivative (2) was used to form the pyrrolering in the target hydrazone molecules. This reaction was then cycled with the corresponding amino acids L-glycine (n = 1) and L-β-alanine (n = 2) to yield the following N-substituted pyrrole carboxylic acids (3 and 4, respectively). According to the process shown in Scheme 1 and detailed in [14,15], the obtained acids were esterified, and then a hydrazinolysis reaction with hydrazine hydrate was carried out to yield the target hydrazide

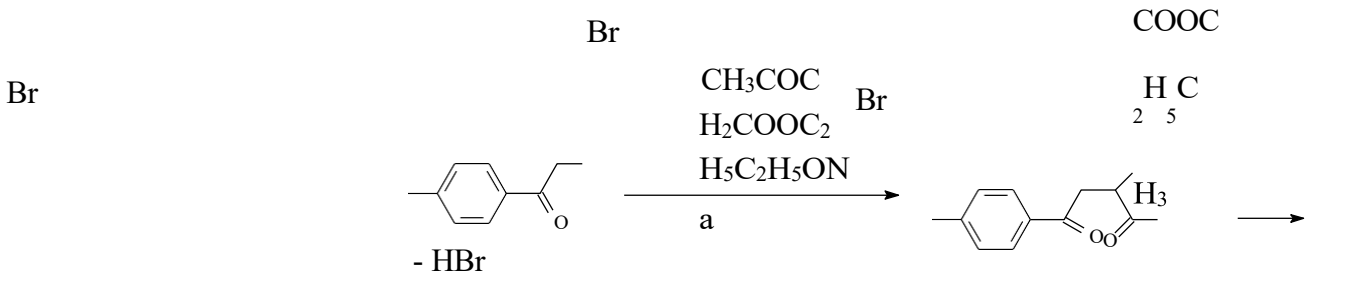

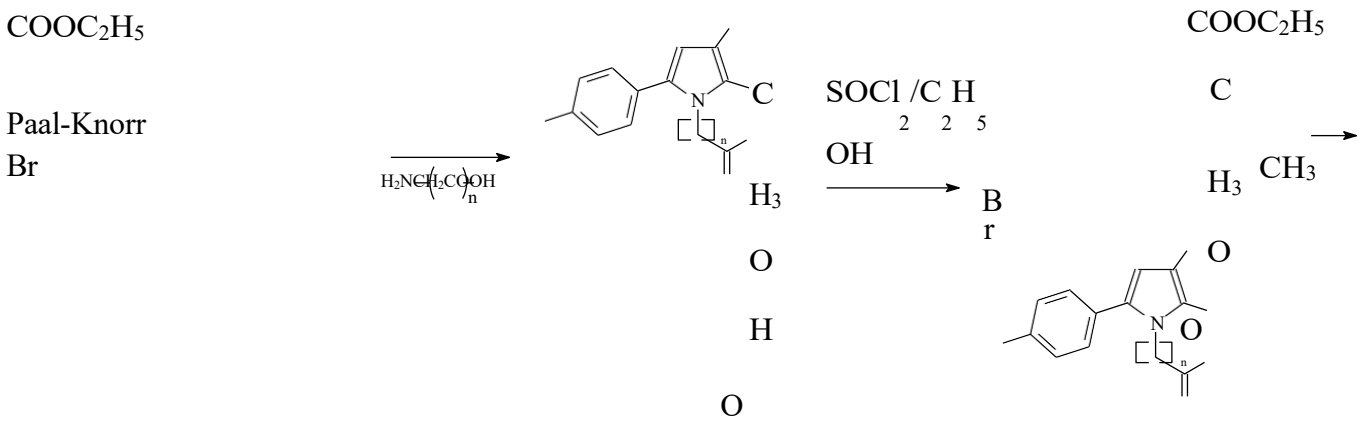

n=1(3)or2(4)

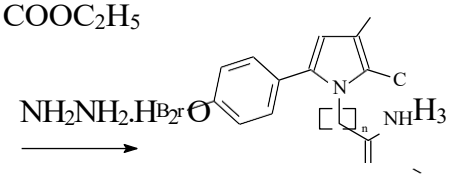

`NH2

O

n=1(7)or 2(8)

Scheme1. Synthesisoftheinitialhydrazides**7**and**8**[14,15].

SynthesisoftheNewN–pyrrolylhydrazide–hydrazones**7a**–**e**and**8a**–**e**

ThenovelseriesofN–pyrrolylhydrazide–hydrazonederivativeswerepreparedun- der microsynthesis scale conditions through condensation reaction from the previously synthesized in our laboratory hydrazides**7**and**8**and the selected carbonyl partners (Figure 2), assuring about 64–86% yield of the purified product. The new compounds were synthesized according to the procedure presented in Scheme 2.

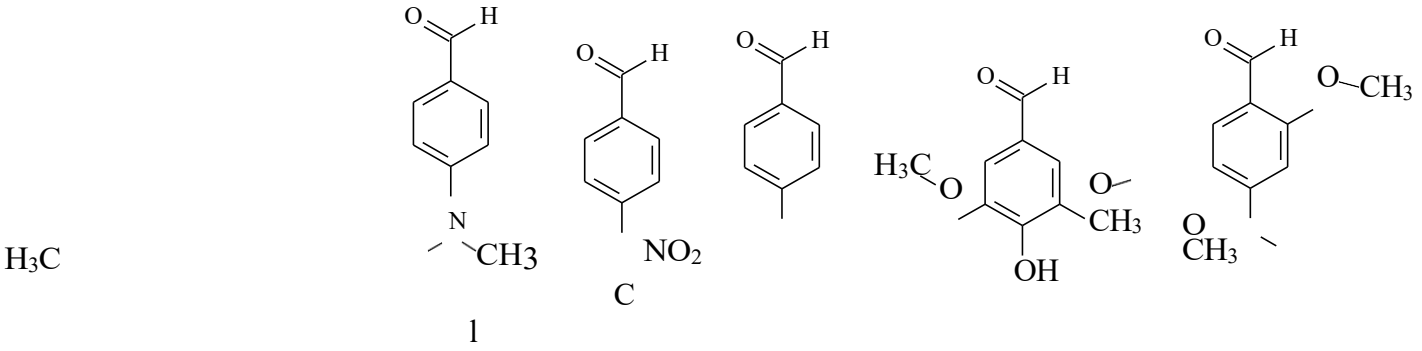

Figure2. Usedaldehydes(**a–e)**.

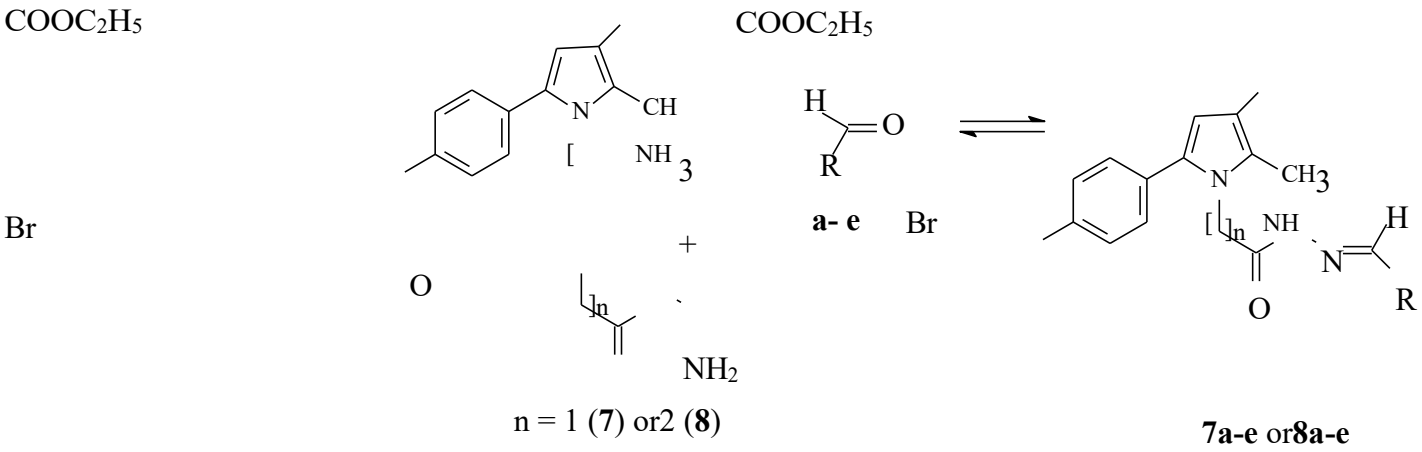

Scheme2. Synthesisofthenewhydrazonecompo unds.

Thereactionconditionswerealtered,aspresentedinTable1,whereintherefluxin glacial acetic acid was selected as the most appropriate.All the new derivativeswere obtained according to that presented in the Materials and Methods section procedures.

Table1. Reactionconditions,reactiontimes,andyields.

ReactionMedia	ReactionTemperature°C	ReactionTime(min)	Yields %
Ethanol	Heating	50–60	46–80
Ethanol+HCl	Roomtemperature	20–30	56–94
Methanol+conc.HCl	Roomtemperature	1440	15–56
Ethanol+glacialaceticacid	100°C	30–50	26–64
Glacialaceticacid	**100°C**	**20–30**	**68–84**

For extended periods of time, the produced pyrrole hydrazones remain stable at room temperature. Melting points, TLC characteristics, IR, and 1H-NMR spectrum data, followed by MS data, were used to clarify the structures of the novel compounds. The novel compounds' consistency with the predicted structure was validated by the spectrum analysis findings. The target derivatives' matching experimental IR, 1H-NMR, and LC-MS spectra are provided as Supplementary Materials.Corresponding elemental studies demonstrated the purity of the derived compounds. According to the IR data, the amide NH group in the molecule of the novel hydrazones has new signals at 3245 cm−1 for the valence asymmetric (vas) vibrations and at 1666 cm−1 (AmideI) and 1533 cm−1 for the eformational (δ) vibrations of the amide NH group (AmideII).Furthermore, the existence of a p-substituted phenyl residue is determined by the formation of a band at around 810 cm−1. A band appears at around 1693–1698 cm−1, indicating the ester group (COOC2H5) at the third position on the core pyrrole ring. The appropriate 1HNMR spectra, where the corresponding groups are accessible at 7.86 ppm for the CH=N group and at 11.38 ppm for the CONH group, respectively, may provide validation of the structural elucidation. The experimental spectral data's acquired values agree with the theoretical ones.

Table 2 provides the matching IDs, melting temperatures, TLC properties, MS data, and yields. The Materials and Methods section contains the corresponding 1H-NMR spectrum data and IR properties.

Table 2.IDs, melting points, TLC characteristics (Rf), MS data, and yields for the new N-pyrrolyl- hydrazones.

IDs	m.p. °C	Rf	MSData $[M+H]^+$(*m/z*)	Yields %
7a	211.4–213.6	0.38	511.13	84
7b	229.4–231.2	0.33	502.05	78
7c	245.9–247.2	0.33	512.07	76
7d	191.9–194.4	0.29	544.10	68
7e	206.0–207.6	0.40	528.11	72
8a	212.0–213.3	0.35	525.15	86
8b	181.4–184.6	0.31	517.06	74
8c	214.4–217.1	0.33	527.09	82
8d	196.6–197.6	0.28	558.12	64
8e	170.0–171.9	0.34	542.13	74

AntioxidantAssays

DPPHRadicalScavengingAssay

The 1,1-diphenyl-2-picrylhydrazyl (DPPH) radical scavenging activity of the newly synthesized derivatives was determined at one concentration—1 mg/mL. Trolox was used as a standard. The obtained results are presented in Figure 3.

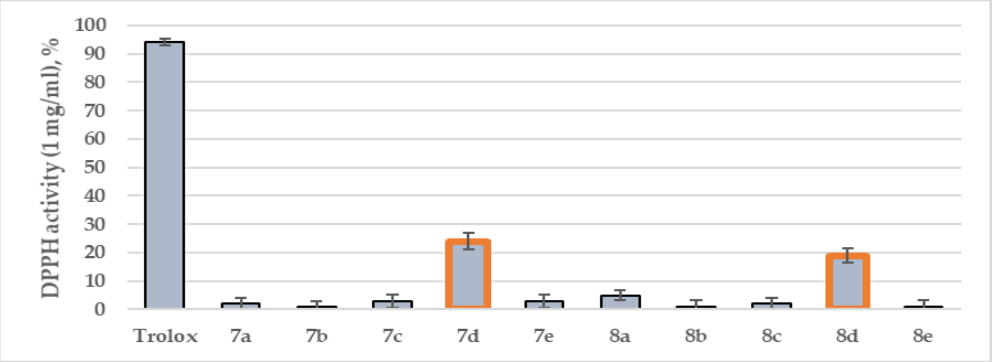

Figure 3. DPPH radical capacities of the newly synthesized compounds **7a**–**e** and **8a**–**e** at concentra-tions of 1 mg/mL. Trolox is used as an internal standard. Data are presented as means from threeindependent experiments. Standard deviation (SD) (n = 3).

The highest DPPH scavenging activity was achieved by compound **7d** (24%).The*β*-alanine hydrazide–hydrazone condensed with the same aldehyde (**8d**) demonstrated similar radical scavenging activity (19%). The standard, Trolox, showed 94% DPPH activity. Therestofthenewlysynthesizedmoleculesdemonstratedweaktonoantioxidanteffects.

ABTSRadicalScavengingAssay

During the 2,2′-azino-bis(3-ethylbenzothiazoline-6-sulphonic acid) (ABTS) assay, the discolorationoftheinitialcolorcouldbedetectedat734nm.TheABTSantioxidantassay of the title compounds is provided in Figure 4.

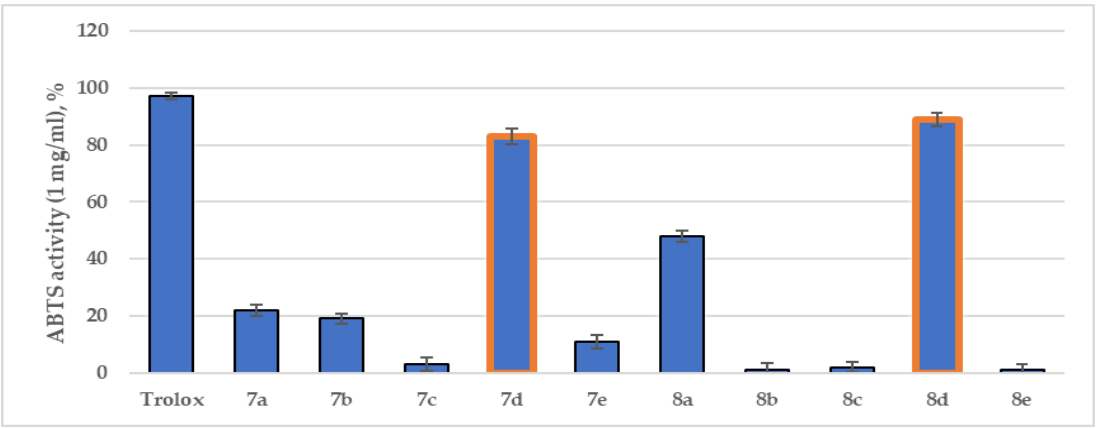

Figure4.ABTStestofthenewlysynthesizedcompounds**7a**–**e**and**8a**–**e**atconcentrationsof1 mg/mL. Trolox is used as an internal standard.Data are presented as means from three inde-pendent experiments. Standard deviation (SD) (n = 3).

DFTCalculations

To rationalize the antioxidant assays and to determine the favored mechanism in- volved in free radical scavenging, density functional theory (DFT) calculations were carried out at the B3LYP/6-311++(d,p) level of theory.

OptimizedGeometries

The most prominent newly synthesized hydrazide–hydrazones (**7d**and**8d**)were selectedforfulloptimizationcalculations.Aninitialconformationalsearchhasbeen

performedbysetting2500iterationswiththeOPLS4forcefield. Thebestsolutionswere further optimized by full DFT geometry optimization at B3LYP/6-311++ (d,p) level of theory. The final geometries of **7d** and **8d** are visualized in Figure 5.

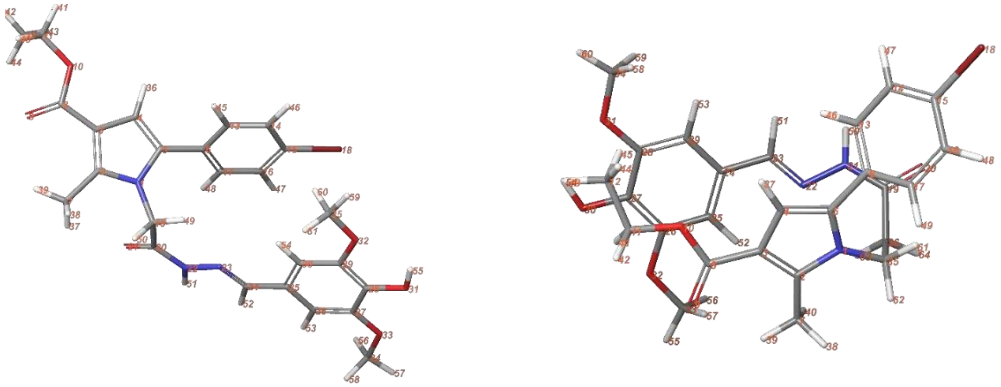

(**a**) (**b**)

Figure 5. Final optimized geometries of the structures with 2500 iterations with OPLS4 force field.The best solutions for (**a**) **7d**; (**b**) **8d** are further optimized at B3LYP/6-311++(d,p).

Overall, 7d and 8d have minimised energies of -4197 and -4157 Hartree, respectively.In structure 7d, the p-bromophenyl moiety was situated in close proximity to the 3,5-dimethoxy-4-hydroxyphenyl fragment, but in structure 8d, the identical groups were in separate places.The p-bromophenyl moiety in the latter example separated from the stable conformation.For more DFT research, the most stable geometries have been chosen as input geometries.Examination of Global Reactivity Descriptors and Frontier Molecular Orbitals (FMOs)

By calculating the highest occupied molecular orbital (HOMO), the lowest unoccupied molecular orbital (LUMO), and then the global reactivity descriptors, including ionisation potential (IP), electron affinity (EA), molecular hardness and softness, electronegativity, and electrophilicity, a quantitative conceptual DFT analysis of the stability and reactivity of the investigated molecules (7d and 8d) was conducted. Figure 6 displays the HOMO-LUMO electronic densities of 7d and 8d that were determined from the optimised structures using DFT/B3LYP/6-311++(d,p) calculations. A positive phase was represented by the colour blue, and a negative phase by the colour red. The HOMO of both ligands was discovered to be primarily located on the pyrrole ring in 7d and 8d, while the LUMO is centred on the 3,5-dimethoxy-4-hydroxyphenyl fragment and the hydrozide–hydrazone moi- ety. The HOMO is further distributed to the hydrazide–hydrazone and the 3,5-dimethoxy-4-hydroxyphenyl moieties as a result of the more compact structure caused by the more energetically favourable conformation of 8d (-4157 Hartree). Using Koopman's theorem for closed-shell compounds, the energies (in atomic units) of the FMOs and the global reactivity descriptors (hardness (η), softness (S), electronegativity (χ), chemical potential (μ), and electrophilicity index (ω)) were computed [16]. Table 3 presents the data.

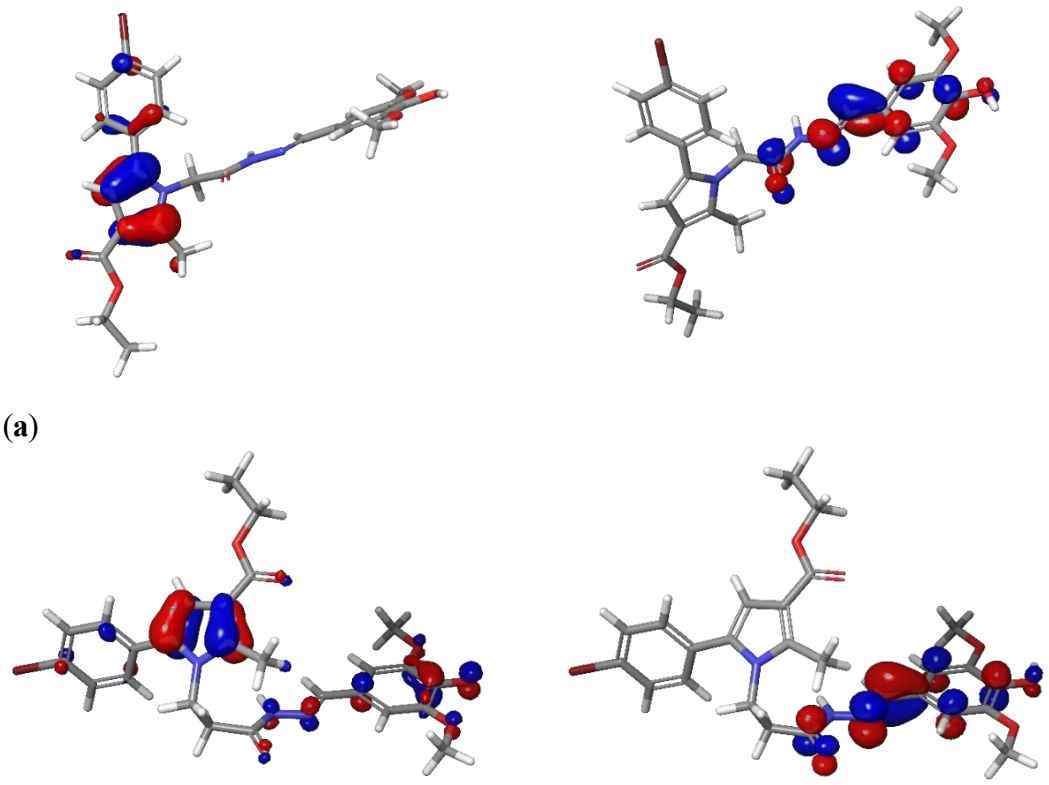

(**a**)

(**b**)

Figure 6.FMOs of **7d** and **8d**, calculated at DFT/B3LYP/6–311++(d,p): (**a**) HOMO and LUMO of **7d;**(**b**) HOMO and LUMO of **8d**.The HOMO-LUMO electronic densities are obtained from the optimized structures with DFT/B3LYP/6–311++(d,p) calculations. Blue color indicates a positive phase, and red indicates a negative phase.

Table 3. FMOs energies and global reactivity descriptors for **7d** and **8d** at B3LYP/6–311++(d,p) levelof theory.

ElectronicParameter	7d	8d
EHOMO	−0.2013	−0.1976
ELUMO	−0.0564	−0.0470
ΔEHOMO−LUMO	0.1449	0.1506
IonizationEnergy(IP)	0.2013	0.1976
ElectronAffinity	0.0564	0.0470
ChemicalHardness	0.0724	0.0753
Softness	6.9060	6.6401
Electronegativity	0.1288	0.1223
ChemicalPotential	−0.1288	−0.1223
ElectrophilicityIndex	0.1145	0.0992

DescriptorsoftheAntioxidantProperties

Thecalculatedvaluesforthedissociationofhydrogen-connectedbondsandtheIPs are provided in Table 4.

Table4. Calculatedbonddissociationenergies(BDEs)andionizationpotentials(IPs)ofthecorre- sponding compounds in gas phase.

Compound	Bond	BDE(Kcal/mol)	IP(Kcal/mol)
7d	O_{31}-H C_7-H N_{22}-H	83.55 90.4 95.10	126.31
8d	O_{30}-H C_7-H N21-H	83.09 88.9 96.2	123.99

InVitroEvaluationsoftheCytotoxicityandAntioxidativeProtectiveActivityontheSH-SY5Y Neuroblastoma Cell Line

EffectsoftheNewlySynthesizedDerivatives**7a**–**e**and**8a**–**e**ontheSH-SY5YCell Viability

The effects of the newly synthesized N-pyrrolyl-hydrazone derivatives on the cellular viability of neuronal SH-SY5Y cells were evaluated, and the corresponding IC50 values were calculated. Inthe current study, the cellswereseeded at density2 $\times 10^4$and were treatedwiththetestcompoundsatconcentrations1–500μMfor24h. Thecalculatedvalues of IC50 are presented in Table 5.

Table 5. Invitro cytotoxicity evaluation of the newly synthesized derivatives**7a**–**e**and**8a**–**e**on SH-SY5Y cells (IC50 values).

CompoundIDs	IC50[μM]	95%ConfidenceIntervals (CI)
7a	55.75	55.65–61.37
7b	67.60	54.31–79.64
7c	>500	NA
7d	99.56	88.87–103.23
7e	63.08	55.56–73.23
8a	56.33	45.25–67.63
8b	57.36	46.26–68.36
8c	58.23	47.36–69.23
8d	57.26	46.29–68.39
8e	91.07	83.65–105-36
Melatonin	>500	NA

The resultsdemonstrated thatcompounds **7c**, **7d**, and**8e**possess lackluster orlow toxicity on human neuronal SH-SY5Y cells, with IC50 of >500 μM, 99.56 μM, and 91.07 μM, respectively.

A model of H2O2-induced oxidative stress in vitro based on the newly synthesised derivatives 7a–e and 8a–ein
The less cytotoxic compounds from the series, 7c, 7d, and 8e, were tested for their potential cell-protective properties against H2O2-induced oxidative stress in SH-SY5Y cells (Figure 7). The cells were pre-incubated for 90 minutes with the investigated drugs at doses of 1, 10, and 20 µM.Due to its well-established neuroprotective properties in a variety of in vitro and in vivo settings, melatonin was utilised as a reference molecule [17].Once the test compounds had been incubated for 90 minutes, SH-SY5Y cells were exposed to H2O2. (1 mM, 15 min), as explained in the section on materials and methods. Compound 7c showed the strongest protection, followed by compounds 7d and 8e.Interestingly, compared to the reference chemical melatonin, both 7c and 7d demonstrated greater protection in all tested doses.It should be mentioned that even at the lowest tested concentration (1 µM), compounds 7e and 7d demonstrated statistically significant protection. Compound 8e's antioxidant protection was weaker.

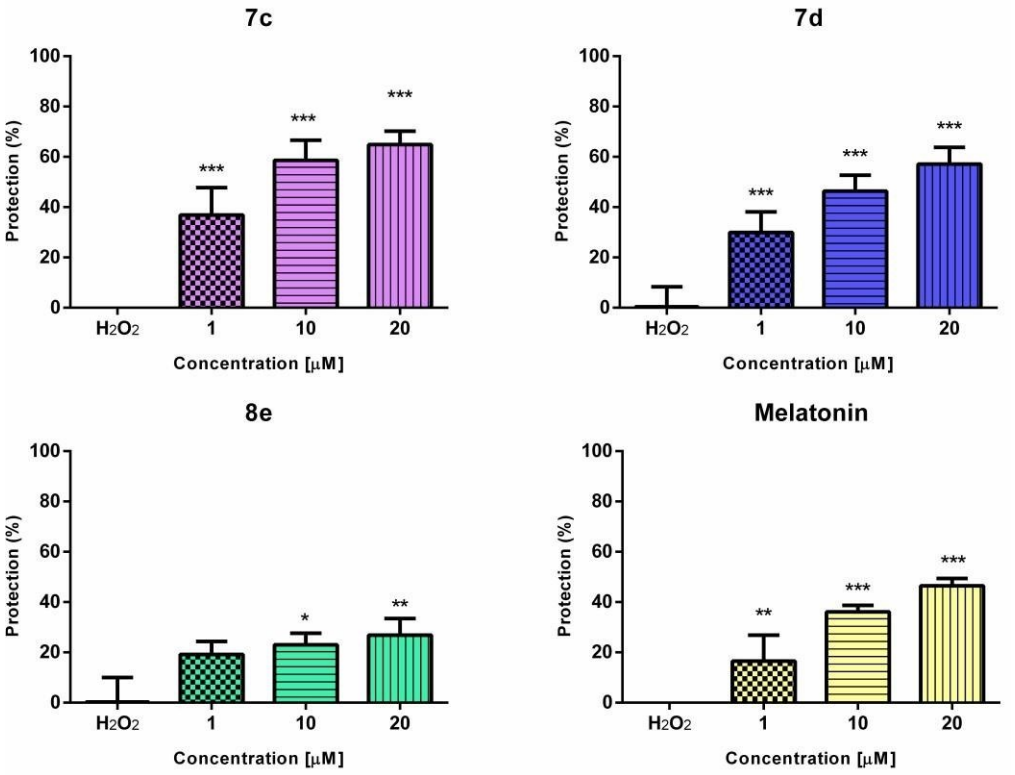

Figure 7. Protective effects of **7c**, **7d**, **8e**, and melatonin in a model of H_2O_2-induced oxidative damage in human neuroblastoma SH-SY5Y cells.Data are presented as means from three independent experiments±SD(n=8). *p<0.05;**p<0.01;***p<0.001,vs. H_2O_2 group(one-wayanalysisof variance with Dunnet's post hoc test).

3. Discussion

Synthesis

Literature demonstrating the relationship between the acidity of the medium and the condensation duration served as the basis for choosing the applicable synthetic approach.The synthesis was first conducted with reaction durations of 50–60 minutes in an ethanol medium without a catalyst [18]. The same reactions were conducted using glacial acetic acid as a catalyst in an ethanol medium in an effort to expedite the procedure.With no discernible change in reaction time, the hydrazones were produced in low yields of 26–64% under these circumstances [19]. As a result, Koopaei provides some information on how carbohydrazides interact with carbonyl compounds in an ethanol medium at a catalyst temperature of 100◦C.It took 20 to 30 minutes to

finish the action under these conditions [20,21].The resulting products underwent recrystallisation and isolation. Neither the yield nor the condensation time were altered by these circumstances.

Therefore, we carried out the synthesis using just lacial aceticacid medium in the present study. This made it possible to obtain pure products in the best time and with good yields (Table 1).

AntioxidantAssays

Two widely used assays for evaluating the antioxidant capabilities of natural and/or synthetic compounds are 1,1-diphenyl-2-picrylhydrazyl (DPPH) and 2,2′-azino-bis(3-ethylbenzothiazoline-6-sulphonic acid) (ABTS). The foundation of both methods is the spectrophotometric determination of the quenching of stable coloured radicals (DPPH or ABTS•+), which enables assessment of antioxidants' capacity to scavenge radicals even in complicated combinations [22].Assay for DPPHRadical Scavenging The DPPH test is among the most widely used assays for assessing antioxidant properties.Its relative affordability is the primary reason for its many uses [23]. The 1,1-diphenyl-2-picrylhydrazyl (DPPH) assay's scavenging action is attributed to antioxidants' capacity to donate hydrogen, as shown by a subsequent drop in absorbance at 517 nm. Single electron transfer (SET) [25], hydrogen atom abstraction (HAT) [24], or mixed mode [26] are the most likely mechanisms of the DPPH test. These mechanisms are connected to the following reaction schemes:

DPPH (violet at 515 nm) + ArOH → DPPHH (colorless) + ArO·HAT (1)

DPPH(violetat515nm)+ArOH→DPPH−(colorless) +ArO·+SET (2)

assuggestedin[27].

This made it feasible for us to use this technique to assess the potential radical scavenging capabilities of the recently produced pyrrole-based hydrazones. Figure 3 displays the findings that were achieved for the target hydrazones.Assay for ABTSRadical Scavenging In the electron-transfer-based ABTS•+radical scavenging test, an antioxidant converts the dark blue 2,2′-azino-bis(3-ethylbenzothiazoline-6-sulfonate) radical cation (ABTS•+) into colourless ABTS, which can be detected spectrophotometrically at 734 nm [28].

Aliterary-basedTwo potential methods of radical scavenging reactions linked to the ABTS test were proposed by comparative analysis: oxidation without coupling and the production of coupling adducts with ABTS•+, which is thought to be more typical for antioxidants of phenolic type. Furthermore, the data indicated that the obtained coupling adducts might undergo additional oxidative degradation, resulting in adducts that resemble hydrazindyilidene and/or imines, with 3-ethyl-2-oxo-1,3-benzothiazoline-6-sulfonate and 3-ethyl-2-imino-1,3-benzothiazoline-6-sulfonate serving as marker compounds, respectively [29].

Given that the structure of the novel pyrrole-based hydrazones contains a phenyl residue, it was interesting to evaluate the target compounds' potential radical scavenging ability as assessed by the two most widely used in vitro antioxidant tests (Figures 3 and 4). Our assessments showed that the ABTS assay showed noticeably higher antioxidant capabilities for the title compounds when compared to the DPPH test. With 89% scavenging activity, 8d was the most notable antioxidant, whilst 7d displayed 83%.The hydrazide-hydrazones that were condensed with 4-dimethylaminobenzaldehyde and 7a and 8a also showed moderate ABTS scavenging capabilities of 22% and 48%, respectively. The ABTS test's capacity to analyse both hydrophobic and hydrophilic chemicals, as well as to evaluate bulky structures, may be the reason for the stark disparities between the two assays [30].Nonetheless, many research teams continue to employ the DPPH test to get meaningful and similar antioxidant data [31]. The presence of a free p-hydroxyl group in the phenyl portion of the structure often results in the greatest radical scavenging action of compounds 7d and 8d.Because of the free electron pair in the N-atom at the p-dimethylamino fragment of the phenyl residue, compounds 7a and 8a seem to have poor radical scavenging characteristics in the ABTS test.Furthermore, 7b, which contains the electron-withdrawing halogen Cl, has a minor impact.The absence of radical scavenging actions in 7e and 8e is linked to the presence of o-methoxy groups in the phenyl residue, most likely because these groups are less prone to form intermolecular hydrogen bonds. Additionally, compared to the lengthier series

8a–e, which is one methylene long, the shorter series 7a–e often exhibits superior radical scavenging activity.The potential of hydrogen atom transfer and/or electron transferability of the active functional groups may be hindered by further conformational modifications.DFT computations

The phenolic O-H bond dissociation enthalpy (BDE), adiabatic ionisation potential (IP), proton dissociation enthalpy (PDE), proton affinity (PA), and electron-transfer enthalpy (ETE) are cited as key factors used to assess the preferred free-radical scavenging pathways of such structures thermodynamically [32]. A number of mechanisms for the free-radical scavenging action of molecules containing phenyl are proposed.Density functional theory (DFT) is the most useful method for calculating these physicochemical descriptors in an attempt to understand these processes [33]. Taking into account recent discoveries, the B3LYP hybrid functional was used to determine the energies of the global reactivity descriptors and the frontier molecular orbitals [32].Information on the energy distribution and energetic behaviour of the 7d and 8d is provided by the matching HOMO and LUMO values.Both compounds' remarkable propensity to donate electrons to empty molecular orbital energy is highlighted by the relatively high negative value of HOMO.Additionally, the compounds' aesthetic stability is established by the negative magnitude of EHOMO and ELUMO [34]. The kinetic stability and chemical reactivity are correlated with the energy gap of the FMOs (EHOMO–ELUMO).For 7d, the estimated border molecular energy gaps are 0.1449 a.u., whereas for 8d, they are 0.1506 a.u. Hard, unreactive, and less polarisable molecules are explained by the wide gap.

The compounds' ability to donate electrons and their reactivity are determined by their chemical softness (S) and hardness (η) values.These characteristics have a direct relationship to chemical reactivity and molecular stability. In contrast, 7d has somewhat less chemical hardness, which translates into less stability. According to the computed softness value, 8 is less favourable in the charge-transfer process.Both ligands' negative chemical potential values (-0.1288 and -0.1223) provide strong stability and resistance to abrupt breakdown into their constituent constituents. The nucleophilicity power is shown by the computed electrophilicity index values (0.1145 and 0.0992 Ha), which are associated with chemical potential and hardness [35]. According to DFT tests, the newly synthesised compounds' best radical scavenging ligands (7d and 8d) are stable, hard, less polarisable, and do not break down into elements. Both compounds have strong electron donation capabilities, according to the HOMO energy. Two processes—hydrogen atom transfer (HAT) and single electron transfer (SET)—were examined in order to investigate the most likely mechanism of antioxidant activity of 7d and 8d. The feasibility of hydrogen donation to the free radical is described by the bond dissociation energies (BDE).It is regarded as one of the most crucial descriptors for figuring out the effects of antioxidants [36].As a result, the BDE was used as the most trustworthy thermodynamic parameter to describe the process of hydrogen atom transfer (HAT). It is anticipated that the weakest O-H bond with the lowest BDE would be more easily absorbed, indicating its better antiradical (antioxidant) action, since this pathway entails the H atom moving from a hydroxyl group of an antioxidant chemical to the free radical.Thus, it will be useful to characterise the compounds' hypothesised antioxidant mechanism by computing the BDEs of the accessible −OH groups in 7d and 8d.The dissociation energies were calculated to determine the activity of the -OH groups in both active ligands and the generation of stable radicals.

Furthermore, in addition to the HAT mechanism, single-electron transfer followed by proton transfer (SET-PT) is another potential route for antioxidant compounds.This process results in the production of a radical cation, which then deprotonates, after an electron is moved from the antioxidant to the free radical. Therefore, the two most crucial factors in characterising the mechanism's viability are the adiabatic ionisation proton (IP) and PDE. Generally speaking, lower IPs are more susceptible to ionisation and electron transfer between antioxidants and free radicals [33]. The conceptual DFT parameters, particularly the IPenergies, are associated with SET [37].The most active compounds are compounds 7d and 8d, according to this order. antioxidants; all other computed IPs were bigger than the reference drug Trolox, indicating that Trolox

had higher action. Radical production occurs at O31, followed by C7 and N21, according to the computationally determined BDE values of all potential dissociation sites in 7d and 8d. Strong N-H bond dissociation in the hydrazide moiety may result in the creation of potential intramolecular stabilisation forces. In both 7d and 8d, the O-H bond is the weakest, indicating the possible HAT mechanism in the exercised antioxidant action. The electron-donation capabilities of the title ligands are caused by the IPs energies.When compared to the BDEs, the previous values of both compounds were greater.Furthermore, the pyrrole-based ligands' very low IP energies [38] suggest that the SET mechanism significantly contributes to their antioxidant capabilities. All things considered, the DFT calculations showed that 7d and 8d had comparable BDE and IP values, which offers a solid theoretical justification for the practical, radical scavenging tests.On SH-SY5Y cells, in vitro cytotoxicity and antioxidant protective activityImpact of the Recently Created Derivatives7a–e and 8a–eonSH-SY5YCell Possibility

The assessment of freshly synthesised compounds' toxicity in various in vitro models is a crucial step in the drug development process.

Because the human neuroblastoma cell line SH-SY5Ya is often used in experimental neuroscience, we chose it as an acceptable model for in vitro neurotoxicity assessment in the present work [39].Because its cells may develop into a wide variety of functioning neurones with the introduction of certain chemicals, this cell line is also a suitable model for simulating different neurodegenerative diseases.Furthermore, because to their sympathetic adrenergic ganglia origin, the SH-SY5Y cells have tyrosine hydroxylase and dopamine-β-hydroxylase activity [39], which makes them suitable for assessing dopamine and serotonin modulations in neurodegeneration. We determined the relevant IC50 values (Table 5) in order to assess the impact of the recently synthesised N-pyrrolyl hydrazone derivatives 7a–e and 8a–e on the cellular survival of the neuronal SH-SY5Y cells. Three compounds with minimal toxicity were identified by the data; compound 7c may be regarded as non-toxic among them, having properties similar to those of melatonin. Interestingly, the findings indicated that a modest increase in cellular toxicity is associated with the extension of the methylene bridge between the core pyrrolering and the one-carbon azomethine fragment of the structure. The compounds from series 8a–e have somewhat greater overall cytotoxicity than those from series 7a–e, according to the measured IC50 values. In particular, derivative 8d's toxicity is 1.7 times greater than that of its monomethyl counterpart, 7d.The compounds 7c, 7d, and 8e were selected for the further antioxidative protection experiment in vitro due to their encouraging safety profile.Impact of the Recently Created Derivatives7a–e and 8a–eina Model of Oxidative Stress Induced by H2O2 in Vitro

The pathophysiology of neurodegenerative disorders and damage to the central nervous system are significantly influenced by oxidative stress [40].High ROS production may overwhelm the body's antioxidant defences, resulting in dangerous circumstances including oxidative stress and damage to cellular structures and functions, when there is an imbalance between the creation of free radicals and detoxification.

Furthermore, excessive formation of free radicals is closely linked to the development of neurodegenerative illnesses and is often thought to have a role in the acute injury of the central nervous system.Numerous factors contribute to the overproduction of free radicals, which directly induce necrotic cell death [43], induction of DNA damage [42], and apoptosis [41] in immature cultured cortical neurones, among other effects [44].

One of the most significant ROS produced by oxidative stress is H2O2. Since it damages several cell components, including proteins, membrane lipids, and nucleic acids, it is often employed as an in vitro model to induce oxidative cell harm [45]. The generation of reactive hydroxyl radicals and the development of Fenton's reaction, which directly interacts with proteins, lipids, and DNA, are the primary mechanisms of oxidative stress induction. The antioxidant protection of the less harmful compounds 7c, 7d, and 8e was evaluated in neuroblastoma SH-SY5Y cells under the H2O2-induced oxidative stress paradigm. As anticipated, SH-SY5Y cell viability was significantly reduced by H2O2-treatment (1 mM, 15 min).Our findings showed that, in comparison to H2O2-treatment, pre-treatment

with compounds 7c, 7d, and 8e greatly boosted the survival of SH-SY5Y cells. All three test drugs including melatonin exhibit dose-dependent protective effects.At all applied doses between 1 and 20 μM, compounds 7c and 7d both exhibit larger protective effects in comparison to the reference substance melatonin, whereas compound 8e has a lesser impact.

Notably, both compounds have comparable in vitro protective effects on peroxide-damaged SH-SY5Y cells, even though 7d has stronger radical scavenging activity than 7c, as demonstrated by the DPPH and ABTS assays. This could suggest that the compounds have pleiotropic modes of antioxidant action in the cells.

The ethyl 5-(4-bromophenyl)-1-(2-(2-(4-hydroxy- 3,5-dimethoxybenzylidene)hydrazine-yl)-2-oxoethyl) was the overall result of the in vitro evaluation of the radical scavenging activity and antioxidative protective effects on neuronal SH-SY5Y cells of the newly synthesised N-pyrrolyl hydrazones.In the H2O2-induced oxidative stress model, -2-methyl-1H-pyrrole-3-carboxylate (7d) is the most promising structure with the lowest cytotoxicity, the strongest radical scavenging activity, and the best antioxidant protection.Restrictions and ConsequencesSection

Since DPPH and ABTS are not physiological radicals, they are not comparable to peroxyl-radicals or other oxygen-based radicals. This is one of the limits of the applicable assays, which also has to do with the specificity of the radical scavenging evaluations utilised. As a result, the test is an indirect technique that relies on lowering persistent radicals. Because light, oxygen, and pH all affect the ultimate absorption, some differences may be seen.In this regard, we want to supplement the conducted cell protection tests on H2O2-induced oxidative stress used here with a few more cellular assessments of the impact of the recently acquired compounds on cell-defined oxidative pathways. These assessments include cellular and subcellular Fe2+ascorbate-induced oxidative stress tests, 6-hydroxydopamine (6-OHDA)-, and tert-butyl hydroperoxide (tBuOOH)-. The results will be published in a subsequent research.

4. MaterialsandMethods

Materials

Thin layer chromatography (TLC) on TLC-Cards Silicagel 60 F254, 1.05554, Merck, Darmstadt, Germany, using CHCl3/CH3CH2OH as a mobile phase, was used to monitor the purity of the compounds obtained and the course of the reactions.An IA 9200 ELECTROTHERMAL apparatus, located at Southend-on-Sea, England, was used to determine melting points in open capillary tubes.The ChemBioDraw Ultra software tool, version 11.0, CambridgeSoft, provides all chemical names in accordance with IUPAC.Using the ATR method and a Smart iTR adaptor, the IRspectrawer was created in the 400–4000 cm−1 range using a NicoletiS10 FT-IR spectrophotometer.A Bruker-Spectrospin WM250 MHz, Faelanden, Switzerland, running at 250 MHz, was used to record 1H-NMR spectra, which were expressed as δ (ppm) in relation to TMS as an internal standard. A 6410 Agilent LCMS triple quadrupole mass spectrometer (LCMS) equipped with an electrospray ionisation (ESI) interface was used to record the mass spectra. A Euro EA 3000-Single, EUROVECTOR SpA analyser was used to conduct elemental analyses.Merck (Darmstadt, Germany) supplied all of the chemicals and reagents used as raw ingredients. Sigma-Aldrich (MerckKGaA, Darmstadt, Germany) provided the RPMI cell culture medium, heat-inactivated foetal bovine serum (FBS), L-glutamine, 3-(4,5-dimethylthiazol-2-yl)-2,5-diphenyl-tetrazoliumbromide (MTT), hydrogen peroxide (H2O2), and dimethylsulfoxide (DMSO), which were required for the pharmacological evaluations.

GeneralSynthesisoftheNewCompounds

The corresponding N-pyrrolyl-carbohydrazide **7** or **8** and any of the carbonyl compounds**a**,**b**,**c**,**d**,or**e**(Figure2)wereincubatedinaglacialacetic acidinaroundbottom flask of 50 mL and stirred at 100 ° Cto complete the reaction under TLC-control.The obtained products were isolated, washed with diethyl ether, and recrystallized, where necessary, by ethanol.

(E)-ethyl5-(4-bromophenyl)-1-(2-(2-(4-(dimethylamino)benzylidene)hydrazinyl)-2- oxoethyl)-2-methyl-1H-pyrrole-3-carboxylate (**7a**)

Yield: 84% as an orange powder; m.p. 211.4–213.6; IR (cm^{-1}): 3245 (NH), 2976 (CH_3 andCH_2),1701($COOC_2H_5$),1666(AmideI),1533(AmideII),1232(C-O),1073(C-N), 810(p-substitutedC_6H_4),552(C-Br);^{1}HNMR(δH,250MHz,$CDCl_3$):1.99[s,3H,CH_2CH_3],

2.54 [s, 3H, CH_3(2)], 3.12–3.15[m, 6H, N(CH_3)2], 4.20–4.24[m, 2H, CH_2CH_3], 4.82[s, 2H, CH_2CO],6.53[s,1H,H(4)],7.19[s,2H,H(3′′),H(5′′)],7.21[s,2H, H(2′′),H(6′′)],7.68–7.69[d, 2H,H(3′),H(5′)],7.88–7.90[d,2H,H(2′),H(6′)],9.99[s,2H,NH-N=CH];LC-MS(ESI):Calc. for$C_{25}H_{28}O_3N_4Br$[M+H]$^+$:511.1339;Found:511.1339.;Anal.Calc.for$C_{25}H_{27}BrN_4O_3$:C, 58.71;H,5.32.Found:C,58.68;H,5.34.

(E)-ethyl5-(4-bromophenyl)-1-(2-(2-(4-chlorobenzylidene)hydrazinyl)-2-oxoethyl)- 2-methyl-1h-pyrrole-3-carboxylate (**7b**)
Yield: 78% as a white powder; m.p. 229.4–231.2; IR (cm^{-1}): 3179 (NH), 2998 (CH_3 and CH_2),1697($COOC_2H_5$),1667(AmideI), 1570(AmideII), 1240(C-O),816 (p-substituted C_6H_4),772(C-Cl),557(C-Br);^{1}HNMR(δH,250MHz,DMSO-d_6):1.25–1.29[m,3H, CH_2CH_3],2.44–2.48[m,3H,CH_3(2)],4.14–4.23[m,2H,CH_2CH_3],5.10[s,2H,CH_2CO], 6.49[s,1H,H(4)],7.23–7.27[m,1H,H(3′′)],7.31–7.36[m,1H,H(5′′)],7.46–7.47[d,1H,H(6′)], 7.50–7.51 [d, 1H, H(2′)], 7.58 [s, 1H, H2′′)], 7.59 [s, 1H, H(6′′)], 7.68 [s, 1H, H(3′)], 7.71 [s, 1H, H(5′)], 8.0 [s, 1H, CH=N], 11.81 [s, 1H, CONH]; LC-MS (ESI): Calc. for $C_{23}H_{22}O_3N_3BrCl$ [M+H]$^+$:502.0527;Found:502.0528.;Anal.Calc.for$C_{23}H_{21}BrClN_3O_3$:C,54.94;H,4.21. Found:C,54.84;H, 4.29.

(E)-ethyl5-(4-bromophenyl)-2-methyl-1-(2-(2-(4-nitrobenzylidene)hydrazinyl)-2- oxo-ethyl)-1H-pyrrole-3-carboxylate (**7c**)
Yield:76%asawhitepowder;m.p.245.9–247.2;IR(cm^{-1}):3201(NH),3064(CH_3 andCH_2),1678($COOC_2H_5$),1592(AmideI),1558(AmideII),1348(NO_2),1240(C-O), 1205(C-N),814(p-substitutedC_6H_4),556(C-Br);^{1}HNMR(δH,250MHz,$CDCl_3$): 1.35–1.37[m,3H,CH_2CH_3],2.58[s,3H,CH_3(2)],4.92[s,2H,CH_2CH_3],5.05[s,2H,CH_2CO], 6.65[s,1H,H(4)],7.58[s,1H,H(5′)],7.59[s,1H,H(3′)],7.78–7.93[m,2H,H(2′),H(6′)], 8.28 [s, 1H, H(2′′)], 8.30 [s, 1H, H(6′′)], 8.40 [s, 1H, H(3′′)], 8.41 [s, 1H, H(5′′)], 10.18 [s, 2H, NH-N=CH]; LC-MS (ESI): Calc. for $C_{23}H_{22}O_5N_4Br$ [M+H]$^+$: 513.0768; Found: 513.0766; Anal.Calc.for $C_{23}H_{21}BrN_4O_5$:C, 53.81; H, 4.12.Found:C, 53.78; H, 4.10.
(E)-ethyl5-(4-bromophenyl)-1-(2-(2-(4-hydroxy-3,5-dimethoxybenzylidene)hydrazine -yl)-2-oxoethyl)-2-methyl-1H-pyrrole-3-carboxylate(**7d**)
Yield:68%asawhitepowder;m.p.191.9-194.4;IR(cm^{-1}):3424(OH),3208(NH), 3067(CH_3 andCH_2),1694($COOC_2H_5$),1673(AmideI),1570(AmideII), 1236(C-O),814 (p-substitutedC_6H_4),554(C-Br);^{1}HNMR(δH,250MHz,DMSO-d_6):1.29[t,3H,CH_2CH_3], 2.47[s,3H,CH_3(2)],3.77[s,6H,OCH_3(3′′),OCH_3(5′′)],4.15–4.21[m,2H,CH_2CH_3], 5.05[s,1H,OH],5.09[s,2H,CH_2CO],6.50[s,1H,H(4)],6.93[s, 1H,H(6′′)],6.98[s, 1H, H(2′′)], 7.28–7.38 [m, 2H, H(3′), H(5′)], 7.59–7.63 [m, 2H, H(2′), H(6′)], 7.89 [s, 1H, CH=N], 11.67 [s, 1H,CONH]; LC-MS (ESI): Calc.for $C_{25}H_{27}O_6N_3Br$ [M+H]$^+$: 544.1078; Found:544.1078;Anal.Calc.for$C_{25}H_{26}BrN_3O_6$:C,55.16;H,4.81.Found:C,55.15;H,4.85.

(E)-ethyl 5-(4-bromophenyl)-1-(2-(2-(2,4-dimethoxybenzylidene)hydrazinyl)-2-oxo- ethyl)-2-methyl-1H-pyrrole-3-carboxylate (**7e**)
Yield: 72% as a white powder; m.p. 206.0–207.6; IR (cm^{-1}): 3234 (NH), 2984 (CH_3 and CH_2), 1698 ($COOC_2H_5$), 1668 (Amide I), 1520 (Amide II), 1240 (C-O), 822 (p-substituted C_6H_4),554(C-Br);^{1}HNMR(δH,250MHz,$CDCl_3$):1.36[t,3H,CH_2CH_3],2.54[s,3H, CH_3(2)],3.93[s,3H,OCH_3(2′′)],3.94[s,3H,OCH_3(4′′)],4.29–4.31[m,2H,CH_2CH_3],4.92[s, 2H,CH_2CO],6.64[s,1H,H(4)],6.47[s,1H,H(3′′)],6.48[s,1H,H(5′′)],7.27[s,1H,H(6′′)], 7.56 [s, 1H, H(2′)], 7.57 [s, 1H, H(6′)], 7.82 [s, 1H, H(3′)], 7.85 [s, 1H, H(5′)], 10.31 [s, 1H, CH=N], 10.32 [s, 1H, CONH]; LC-MS (ESI): Calc.for $C_{25}H_{27}O_5N_3Br$ $[M+H]^+$: 528.1129; Found:528.1132;Anal.Calc.for$C_{25}H_{26}BrN_3O_5$:C,56.83;H,4.96.Found:C,56.84;H,4.98.

(E)-ethyl5-(4-bromophenyl)-1-(3-(2-(4-(dimethylamino)benzylidene)hydrazinyl)-3- oxopropyl)-2-methyl-1H-pyrrole-3-carboxylate (**8a**)
Yield: 86% as a white powder; m.p.212.0–213.3; IR (cm^{-1}): 3266 (NH), 2907 (CH_3 and CH_2), 1693 ($COOC_2H_5$), 1668 (Amide I), 1570 (Amide II), 1265 (C-N), 1249 (C-O), 831(p-substitutedC_6H_4),554(C-Br);^{1}HNMR(δH,250MHz,$CDCl_3$):1.27[s,3H,CH_2CH_3], 2.54[s,3H,CH_3(2)],2.59–2.62[m,2H,CH_2CH_2CO],3.12[s,3H,$N(CH_3)$],3.14[s,3H, $N(CH_3)$],4.17–4.19[m,2H,CH_2CH_2CO],4.27–4.28[m,2H,CH_2CH_3],6.49[s,1H,H(4)], 7.18–7.19[m,2H,H(3′′),H(5′′)],7.45–7.49[m,2H,H(2′′),H(6′′)],7.67–7.69[d,2H,H(3′), H(5′)], 7.95–7.96 [d, 2H, H(2′), H(6′)], 8.60 [s, 1H, CH=N], 9.97 [s, 1H, CONH]; LC-MS (ESI): Calc.for $C_{26}H_{30}O_3N_4Br$ $[M+H]^+$: 525.1496; Found: 525.1504; Anal.Calc.for $C_{26}H_{29}BrN_4O_3$: C,59.43;H,5.56. Found: C,59.23;H,5.66.

(E)-ethyl5-(4-bromophenyl)-1-(3-(2-(4-chlorobenzylidene)hydrazinyl)-3-oxopropyl) -2-methyl-1H-pyrrole-3-carboxylate(**8b**)
Yield: 74% as a white powder; m.p. 181.4–184.6; IR (cm^{-1}): 3282 (NH), 2931 (CH_3 and CH_2),1698($COOC_2H_5$),1668(AmideI), 1571(AmideII), 1252(C-O),813 (p-substituted C_6H_4),771(C-Cl),560(C-Br);^{1}HNMR(δH,250MHz,DMSO-d_6):1.23–1.27[m,3H, CH_2CH_3],2.61[s,3H,CH_3(2)],2.83[t,2H,CH_2CH_2CO],4.13–4.16[q,2H,CH_2CH_2CO], 4.24–4.33[q,2H,CH_2CH_3],6.41[s,1H,H(4)],7.35–7.37[d,2H,H(3′′),H(5′′)],7.51–7.53[d, 2H, H(2′′), H(6′′)], 7.56–7.60 [m, 2H, H(2′), H(6′)], 7.61–7.63 [d, 1H, H(3′)], 7.69–7.71 [d, 1H, H(5′)], 7.86 [s, 1H, CH=N], 11.38 [s, 1H, CONH]; LC-MS (ESI): Calc. for $C_{24}H_{24}O_3N_3BrCl$ $[M+H]^+$:516.0684;Found:516.0684;Anal.Calc.for$C_{24}H_{23}BrClN_3O_3$:C,55.78;H,4.49. Found:C,55.76;H, 4.48.

(E)-ethyl5-(4-bromophenyl)-2-methyl-1-(3-(2-(4-nitrobenzylidene)hydrazinyl)-3- oxopropyl)-1H-pyrrole-3-carboxylate (**8c**)
Yield:82%asayellowpowder;m.p.214.4–217.1;IR(cm^{-1}):3294(NH),2929(CH_3 andCH_2),1689($COOC_2H_5$),1658(AmideI),1572(AmideII),1512(NO_2),1340(C-N), 1249(C-O),814(p-substitutedC_6H_4),558(C-Br);^{1}HNMR(δH,250MHz,$CDCl_3$):1.26–1.29[m,3H,CH_2CH_3],2.55[s,3H,CH_3(2)],2.61[t,2H,CH_2CH_2 CO],4.18–4.20[m,2H, CH_2CH_2CO],4.21–4.25[m,2H,CH_2CH_3],6.49[s,1H,H(4)],7.17[s,1H,H(3')],7.18[s ,1H, H(5')],7.48[s,1H,H(6')],7.49[s,1H,H(2')],8.00[s,1H,H(2′′)],8.02[s,1H,H(6′′)],8.34[s, 2H,H(3′′),H(5′′)],10.09[s,2H,NH-N=CH];LC-MS(ESI):Calc.for$C_{24}H_{24}O_5N_4Br[M+H]^+$: 527.0925;Found:527.0927;Anal.Calc.for$C_{24}H_{23}BrN_4O_5$:C, 54.66;H,4.40.Found:C, 54.64;H,4.39.

(E)-ethyl 5-(4-bromophenyl)-1-(3-(2-(4-hydroxy-3,5-dimethoxybenzylidene) hydra zine-yl)-3-oxopropyl)-2-methyl-1H-pyrrole-3-carboxylate (**8d**)
Yield: 64%asawhitepowder;m.p.196.6–197.6;IR(cm^{-1}): 3422(OH),3278(NH), 2971(CH_3 andCH_2),1693 ($COOC_2H_5$), 1666(AmideI),1574 (AmideII),1250 (C-O),814 (p-substituted C_6H_4), 551 (C-Br);^{1}HNMR (δH, 250 MHz, DMSO-d_6): 1.22–1.27 [m, 3H, CH_2CH_3],2.61[t,2H,CH_2CH_2CO],2.64[s,3H,CH_3(2)],3.78[s, 6H,OCH_3(3′′),OCH3(5′′)], 4.12–4.16[m,2H,CH_2CH_2CO],4.20–4.26[m,2H,CH_2CH_3],6.41[s,1H,H(4)],6.80[s,1H,

OH], 7.36–7.38 [m, 2H, H(2″), H(6″)], 7.54–7.56 [m, 2H, H(3′), H(5′)], 7.62–7.64 [m, 2H, H(2′), H(6′)], 7.78 [s, 1H, CH=N], 11.20 [s, 1H,CONH]; LC-MS (ESI): Calc.for $C_{26}H_{29}O_6N_3Br$ [M+H]$^+$:558.1234;Found:558.1243;Anal.Calc.for$C_{26}H_{28}BrN_3O_6$:C,55.92;H,5.05. Found:C,55.98;H, 5.02.

(E)-ethyl5-(4-bromophenyl)-1-(3-(2-(2,4-dimethoxybenzylidene)hydrazinyl)-3- oxopropyl)-2-methyl-1H-pyrrole-3-carboxylate (**8e**)
Yield: 74% as a white powder; m.p. 170.0–171.9; IR (cm^{-1}): 3298 (NH), 2968 (CH_3 and CH_2), 1692 ($COOC_2H_5$), 1673 (Amide I), 1571 (Amide II), 1253 (C-O), 813 (p-substituted C_6H_4),549(C-Br); ^{1}HNMR(δH,250MHz,$CDCl_3$):1.24–1.28[m,3H,CH_2CH_3],2.54[s,3H, CH_3(2)],2.58–2.63[m,2H,CH_2CH_2CO],3.18[s,3H,OCH_3(4″)],3.83[s,3H,O CH_3(2″)], 4.18–4.20 [m,2H,CH_2CH_2CO],4.21–4.23[m,2H,CH_2CH_3],6.37–6.68[d,1H, H(3″)],6.47–6.48[m,1H,H(5″)],6.49[s,1H,H(4)],7.14[s,1H,H(3′)],7.18 [s,1H,H(5′)],7.48[s,1H, H(6′)],7.49[s,1H,H(2′)],7.73–7.76[d,1H,H(6″)],8.34[s,1H,CH=N],10.22[s,1H,CONH]; LC-MS (ESI): Calc. for $C_{26}H_{29}O_5N_3Br$ $[M+H]^+$: 542.1285; Found: 542.1293; Anal. Calc. for $C_{26}H_{28}BrN_3O_5$: C, 57.57; H, 5.20. Found: C, 57.55; H, 5.22.

AntioxidantActivityEvaluation

DPPHRadicalScavengingAssay

The scavenging assay of the title compounds against DPPH radical was carried out by the widely employed protocol of Brand-Williams et al. [46].Briefly, a single concentrationof 1 mg/mL for each synthesized compound in methanol was obtained.Subsequentaddition of 1 mL of the methanol solution of DPPH (1 mmol/L) was performed.Thereactionmixtureswereincubatedinthedarkfor30min.Theabsorbancewasmeasured at 517 nm.Three measurements were carried out for each sample; 6-Hydroxy-2,5,7,8- tetramethylchroman-2-carboxylic acid (Trolox) was applied as a standard. The percentage inhibition of the tested samples was calculated by the following Formula (3):

$$DPPH_{scavengingactivity}=Abs_{control}-Abs_{sample}/Abs_{control}\times 100\% \quad (3)$$

where $Abs_{control}$ is the absorbance of the DPPH radical in methanol, and Abs_{sample} is the absorbance of the DPPH radical solution mixed with the sample.

ABTSRadicalScavengingAssay

TheABTSradicaltestsweremeasuredaccordingtoamodifiedmethodofArnao etal.[47].Thetestsolutionsweredissolvedinmethanol(1mg/mL)atambienttemperature. The radical cation of ABTS ($ABTS^{+\bullet}$) was created by mixing 7 mmol/L solution of ABTS and2.4mmol/Lsolutionofpotassiumpersulphate,whichweresettoreactfor14hinthe darkatroomtemperature. Theworkingsolutionsconsistedof2mLofthestocksolution diluted in 50 mL of methanol with an absorbance of 0.294 ±0.05 units at 734 nm.Then, 1 mL of the ABTS working solution was allowed to react with the title compounds for10 min, with a subsequent absorbance determination.The inhibition percentages were evaluated by applying the same formula as the DPPH assay (4).

$$ABTS_{scavengingactivity}=Abs_{control}-Abs_{sample}/Abs_{control}\times 100\% \quad (4)$$

where $Abs_{control}$ is the absorbance of the ABTS radical in methanol, and Abs_{sample} is the absorbance of the ABTS radical solution mixed with the sample.

DFTTheoreticalCalculations

All of the theoretical computations were carried out by applying Jaguar [48].The initial geometries for the DFT calculations were achieved after a conformational search with 2500 iterations and OPLS4 force field.Subsequently, full geometry optimizations ofthebestconformationsofcompounds**7d**and**8d**withBecke'sthree-parameterhybrid exchange–

wereperformed.
Itwasfoundthatoutof11functionsand14basissets,themostoptimal combinationintermsofbothaccuracyandresourceusageforbonddissociationenergies calculations is M06-2X/6-311G(d,p) [49].The frontier molecular orbitals and the global reactivitydescriptorswerecalculatedatthesamelevelofthe ory. Thebonddissociation energies wereobtainedwithM06–2Xand6–311Gbasis setconsideringarecentreport[49].

InVitroPharmacologicalEvaluations

Cell Line

Human neuroblastoma cell line SH-SY5Y was purchased from European Collection ofCellCultures(ECACC,Salisbury,UK).SH-SY5YcellswerecultivatedinanRPMI 1640mediumsupplementedwith10%heat-inactivatedFBS,2mML-glutamine,and1% antibiotics(penicillin/streptomycin).

Thecelllinewasincubatedat37 ˚ Cwith5%ofCO_2, and the culture's medium was replaced with a time interval of 2–3 days.

CellViabilityAssay

To achieve confluence, the SH-SY5Y cells were plated for 24hat37◦Con96-well plates at a density of 2 ×104 cells per well. The chemicals (1–500 µM) were applied to the cells after a 24-hour period. The MTT test was used to measure live cells' metabolic activity. The water-soluble, yellow-colored tetrazolium salt MTT (3-(4,5-dimethylthiazol2-yl)-2,5-diphenyltetrazolium bromide) was converted to a purple, insoluble formazan crystal by the mitochondrial succinate dehydrogenase system of live cells.The MTT solution (10 mg/mL in PBS) was added to each well after the cells had been cultured with the test solutions for 24 hours. The combination was then incubated at 37 °C for three hours.Following a thorough aspiration of the MTT solution, 100 mL of DMSO was added to dissolve the formazan crystals that were produced.A multiplate reader Synergy 2 (BioTek Instruments, Inc., Highland Park, Winooski, VT, USA) was used to measure the optical density between 570 and 690 nm in order to assess the cell viability [50].

H_2O_2-InducedOxidativeStressModelinSH-SY5YCells

SH-SY5Y cells were seeded in 96-well plates at a density of 3.5 × 104/well in 100 µL for 24 hours in order to create the H2O2-induced oxidative stress paradigm. Following the aspiration of the cell media, the cells were subjected to varying concentrations of the tested chemicals (1, 10, and 20 µM) for 90 minutes. The cells were then rinsed with phosphate-buffered saline (PBS) and exposed to the oxidative stress (H2O21mMin PBS, 15 minutes).The culture medium was used to alter the contents of every well.The MTT test was used to measure the quantity of adherent live cells after 24 hours.Cells treated with hydrogen peroxide were seen as having 0% protection, whereas negative controls, or cells not treated with hydrogen peroxide, were regarded as having 100% protection.

StatisticalAnalysis

GraphPad Prism 6 software has been used to do statistical analysis on the data. Every experiment was conducted in triplicate, and the mean ±SD (n = 8) was used to present the data. Using Dunnet's multiple comparisons post-test and one-way ANOVA, group comparisons have been carried out. To confirm the importance of the observed discrepancies, we conducted statistical analysis on the data. Group differences were deemed significant if they were $p<0.05$, $p<0.01$, and $p<0.001$.

5. Conclusions

We synthesised ten novel N-pyrrolyl hydrazide–hydrazones. The novel compounds' structure was clarified using the proper IR, 1H-NMR, and MS spectrum data. The matching melting temperatures, TLC properties, and elemental tests demonstrated the compounds' purity. According to DFT investigations, the newly synthesised compounds' best radical scavenging ligands (7d and 8d) are stable molecules that don't break down intoelements, have a harsh character, and are less polarisable. Both compounds have strong electron donation capabilities, according to the HOMO energy. All things considered, 7d and 8d may easily scavenge free radicals in the biological system by single electron transfer and hydrogen atom donation. The human neuroblastoma cell line SH-SY5Y was used for in vitro neurotoxicity, cellular toxicity, and cell protection evaluations. The results showed that this cell line was the most promising, with the lowest toxicity and the maximum antioxidant protection.

References

1. Singh,S.;Singh,R.P.Invitromethodsofassayofantioxidants:Anoverview.*FoodRev.Int.***2008**,*24*,392–415.[CrossRef]
2. Linseman,D.A.Targetingoxidativestressforneuroprotection.*Antioxid.RedoxSignal.***2009**,*11*,421–424.[CrossRef][PubMed]
3. Cho, K.S.; Shin, M.; Kim, S.; Lee, S.B. Recent advances in studies on the therapeutic potential of dietary carotenoids in neurode-generative diseases. *Oxid. Med. Cell. Longev.* **2018**, *2018*, 4120458. [CrossRef] [PubMed]
4. Thurkauf, A.; Yuan, J.; Chen, N.; Wasley, J.W.; Meade, R.; Woodruff, K.H.; Ross, P.C. 1-Phenyl-3-(aminomethyl) pyrroles as potentialantipsychoticagents.Synthesisand dopaminereceptorbinding.*J.Med.Chem.***1995**,*38*,4950–4952.[CrossRef]
5. de Oliveira, K.N.; Costa, P.; Santin, J.R.; Mazzambani, L.; Bürger, C.; Mora, C.; Nunes, R.J.; de Souza, M.M. Synthesis and antidepressant-likeactivityevaluationofsulphonamidesand sulphonyl-hydrazones.*Bioorg.Med.Chem.***2011**,*19*,4295–4306. [CrossRef]
6. Ragavendran, J.V.; Sriram,D.; Patel,S.K.; Reddy,I.V.; Bharathwajan,N.; Stables,J.; Yogeeswari,P.Designandsynthesisof anticonvulsants from a combined phthalimide–GABA–anilide and hydrazone pharmacophore.*Eur. J. Med. Chem.* **2007**, *42*,146–151.[CrossRef]
7. Zlatanova, H.; Vladimirova, S.; Kandilarov, I.; Kostadinov, I.; Delev, D.; Kostadinova, I.; Bijev, A. Analgesic effect of a newly synthesized N-pyrrolylcarboxylic acid in experimental conditions. *Europ. Neuropsychopharmacol.* **2019**, *29*, S468–S469. [CrossRef]
8. MacLean,P.D.;Chapman,E.E.;Dobrowolski,S.L.;Thompson,A.;Barclay,L.R.C.Pyrrolesasantioxidants: Solventeffectsandthe nature of the attacking radical on antioxidant activities and mechanisms of pyrroles, dipyrrinones, and bile pigments.*J.Org. Chem.***2008**,*73*,6623–6635.[CrossRef]
9. Bhosale, J.D.; Dabur, R.; Jadhav, G.P.; Bendre, R.S. Facile syntheses and molecular-docking of novel substituted 3,4-dimethyl- 1H-pyrrole-2-carboxamide/carbohydrazideanalogueswithantimicrobialandantifungalproperties.*Molecules***2018**,*23*,875. [CrossRef]
10. Peng, Z.; Wang, G.; Zeng, Q.H.; Li, Y.; Wu, Y.; Liu, H.; Wang, J.J.; Zhao, Y. Synthesis, antioxidant and anti-tyrosinase activity of 1,2,4-triazole hydrazones as antibrowning agents. *FoodChem.* **2021**, *341*, 128265. [CrossRef]
11. Boulebd,H.;Zine,Y.;Khodja,I.A.;Mermer, A.;Demir,A.;Debache,A.Synthesisandradicalscavengingactivityofnewphenolic hydrazone/hydrazidederivatives:Experimentalandtheoreticalstudies.*J.Mol.Struct.***2022**,*1249*,131546.[CrossRef]

12. Khodja,A.;Bensouici,C.;Bouleb,H.Combinedexperimentalandtheoreticalstudiesofthestructure-antiradicalactivityrelationshipofheterocyclichydrazonecompounds.*J.Mol.Struct.***2020**,*1221*,128858.[CrossRef]
13. Tzankova, D.G.; Vladimirova, S.P.; Peikova, L.P.; Georgieva, M.B. Synthesis and preliminary antioxidant activity evaluation of newpyrrolebasedarylhydrazones.*Bulg.Chem.Commun.***2019**,*51*,179–185.
14. Bijev, A.;Georgieva,M.Pyrrole-basedhydrazonessynthesizedandevaluatedinvitroaspotentialtuberculostatics. *Lett. Drug Des.Discov.***2010**,*7*,430–437.[CrossRef]
15. Georgieva,M.;Bijev,A.;Prodanova,P.Synthesisandcomparativestudyoftuberculostaticactivityofpyrrole-basedhydrazonesrelated to structural variations. *Pharmacia* **2010**, *52*, 3–14.
16. Tsuneda,T.;Song,J.W.;Suzuki,S.;Hirao,K.On Koopmans'theoremindensityfunctionaltheory. *J. Chem.Phys.***2010**,*133*,174101. [CrossRef]
17. Zhang, Y.; Chen, D.; Wang, Y.; Wang, X.; Zhang, Z.; Xin, Y. Neuroprotective effects of melatonin-mediated mitophagy through nucleotide-bindingoligomerizationdomainandleucine-richrepeat-containingproteinX1inneonatalhypoxic–ischemicbrain damage.*FASEBJ.***2023**,*37*,e22784. [CrossRef]
18. Joshi, S.D.; Kumar, D.; Dixit, S.R.; Tigadi, N.; More, U.A.; Lherbet, C.; Aminabhavi, T.M.; Yang, K.S. Synthesis, characterization andantitubercularactivitiesofnovelpyrrolylhydrazonesandtheirCu-complexes. *Eur. J.Med. Chem.* **2016**,*121*,21–39. [CrossRef]
19. Manvar, A.; Bavishi, A.; Radadiya, A.; Patel, J.; Vora, V.; Dodia, N.; Rawal, K.; Shah, A. Diversity oriented design of various hydrazidesandtheirinvitroevaluationagainstMycobacteriumtuberculosisH37Rvstrains .*Bioorg.Med.Chem.Lett.***2011**,*21*, 4728–4731. [CrossRef]
20. Nassiri, K.M.; Assarzadeh, M.J.; Almasirad, A.; Ghasemi-Niri, S.F.; Amini, M.; Kebriaeezadeh, A.; Nassiri, K.N.; Ghadimi, M.; Tabei,A.Synthesisandanalgesicactivityofnovelhydrazideandhydrazinederivatives. *Iran.J.Pharm.Res.***2013**,*12*,721–727.
21. Rawat,P.;Singh,R.N.Synthesis,spectralandchemicalreactivityanalysisof2,4-dinitrophenylhydrazonehavingpyrrolemoiety. *J.Mol.Struct.* **2015**,*1097*,214–225.[CrossRef]
22. Sujarwo, W.; Keim, A.P. Spondias pinnata (L. f.) Kurz. (Anacardiaceae): Profiles and Applications to Diabetes. In *Bioactive Food as Dietary Interventions for Diabetes*, 2nd ed.; Elsevier Inc.:Amsterdam, The Netherlands, 2019; ISBN 978-0-12-813822-9.[CrossRef]
23. Kedare,S.B.;Singh,R.P.Genesisanddevelopmentof DPPHmethodofantioxidantassay.*J.FoodSci.Technol.***2011**,*48*,412–422. [CrossRef] [PubMed]
24. Dawidowicz,A.L.;Olszowy,M.;Józ´wik-Dole¸ba,M.ImportanceofsolventassociationintheestimationofantioxidantpropertiesofphenoliccompoundsbyDPPHmethod. *J.FoodSci.Technol.***2015**,*52*,4523–4529. [CrossRef]
25. Brizzolari, A.; Foti, M.C.; Saso, L.; Ciuffreda, P.; Lazarevic´, J.; Santaniello, E. Evaluation of the radical scavenging activity of somerepresentative isoprenoid and aromatic cytokinin ribosides (N6-substituted adenosines) by in vitro chemical assays.*Nat. Prod.Res.***2022**, *36*, 6443–6447. [CrossRef]
26. Schaich, K.M. Lipid oxidation in specialty oils.In *NutraceuticalandSpecialtyOils*; Shahidi., F., Ed.; CRC Press/Taylor &Francis: London,UK,2006;pp.401–448.
27. Amarowicz, R.; Pegg, R.B. Functional Food Ingredients from Plants.In *Advances in Food and Nutrition Research*; Elsevier Inc.: Amsterdam, The Netherlands, 2019.
28. Dasgupta, A.; Klein, K. Methods for Measuring Oxidative Stress in the Laboratory.In*Antioxidants in Food, Vitamins and Supplements*; Elsevier Inc.: Amsterdam, The Netherlands, 2014. [CrossRef]
29. Ilyasov,I.R.;Beloborodov,V.L.;Selivanova,I.A.;Terekhov,R.P.ABTS/PPDecolorizationassayofantioxidantcapacityreaction pathways.*Int. J.Mol. Sci.* **2020**,*21*,1131. [CrossRef]

30. Mateev,E.;Georgieva,M.;Zlatkov,A.Design,microwave-assistedsynthesis,biologicalevaluation,molecular docking,andadme studiesofpyrrole-basedhydrazide-hydrazonesaspotentialantioxidantagents.*Maced.J.Chem.Chem.Eng.***2022**,*41*,175–186.[CrossRef]
31. Munteanu, I.G.; Apetrei, C. Analytical methods used in determining antioxidant activity: A Review. *Int. J. Mol. Sci.* **2021**, *22*, 3380.[CrossRef] [PubMed]
32. Leopoldini, M.; Russo, N.; Toscano, M. The molecular basis of working mechanism of natural polyphenolic antioxidants. *Food Chem.***2011**,*125*,288–306.[CrossRef]
33. Farrokhnia,M.DensityFunctionalTheoryStudiesontheAntioxidantMechanismandElectronicPropertiesofSomeBioactive Marine Meroterpenoids:Sargahydroquionic Acid and Sargachromanol.*ACSOmega***2020**, *5*, 20382–20390.[CrossRef]
34. Safna Hussan, K.P.; Shahin Thayyil, M.; Rajan, V.K.; Muraleedharan, K. DFT studies on global parameters, antioxidant mechanismand molecular docking of amlodipine besylate.*Comput. Biol. Chem.* **2019**, *80*, 46–53.[CrossRef]
35. Choudhary, V.K.; Bhatt, A.K.; Dash, D.; Sharma, N. DFT calculations on molecular structures, HOMO–LUMO study, reactivity descriptors and spectral analyses of newly synthesized diorganotin (IV) 2-chloridophenylacetohydroxamate complexes.*J.Comput. Chem.***2019**,*40*,2354–2363.[CrossRef][PubMed]
36. Dávalos, J.Z.; Valderrama-Negrón, A.C.; Barrios, J.R.; Freitas, V.L.S.; Ribeiro da Silva, M.D.M.C. Energetic and structural propertiesoftwophenolicantioxidants:Tyrosolandhydroxytyrosol.*J.Phys.Chem.A***2018**,*122*,4130–4137.[CrossRef][PubMed]
37. Liang,N.;Kitts,D.D.Antioxidantpropertyofcoffeecomponents:Assessmentofmethodsthatdefinemechanismsofaction.*Molecules***2014**,*19*,19180–19208.[CrossRef]
38. Lu, L.; Qiang, M.; Li, F.; Zhang, H.; Zhang, S. Theoretical investigation on the antioxidative activity of anthocyanidins:A DFT/B3LYP study. *Dyes Pigment.* **2014**, *103*, 175–182. [CrossRef]

39. Lopez-Suarez, L.; Al Awabdh, S.; Coumoul, X.; Chauvet, C. The SH-SY5Y human neuroblastoma cell line, a relevant in vitro cell model for investigating neurotoxicology in human:Focus on organic pollutants.*Neurotoxicology***2022**, *92*, 131–155.[CrossRef]
40. Wang,X.;Zhou,Y.;Gao,Q.;Ping,D.;Wang, Y.;Wu,W.;Lin,X.;Fang,Y.;Zhang,J.;Shao, A.TheRoleofexosomalmicroRNAs and oxidative stress in neurodegenerative diseases. *Oxid. Med. Cell. Longev.* **2020**, *2020*, 3232869. [CrossRef]
41. Ratan,R.R.;Murphy,T.H.;Baraban,J.M.Oxidat ivestressinducesapoptosisinembryoniccortical neurons.*J. Neurochem.***1994**,*62*, 376–379.[CrossRef]
42. Floyd, R.A.; Carney, J.M. Free radical damage to protein and DNA: Mechanisms involved and relevant observations on brain undergoingoxidativestress.*Ann.Neurol.***19 92**,*32*(Suppl. S1),S22–S27.[CrossRef]
43. Kane, D.J.; Sarafian, T.A.; Anton, R.; Hahn, H.; Gralla, E.B.; Valentine, J.S.; Ord, T.; Bredesen, D.E. Bcl-2 inhibition of neural death:Decreased generation of reactive oxygen species. *Science* **1993**, *262*, 1274–1281. [CrossRef]
44. Amoroso,S.;Gioielli,A.;Cataldi,M.;DiRenzo, G.;Annunziato,L.IntheneuronalcelllineSH-SY5Y,oxidativestress-inducedfree radical overproduction causes cell death without any participation of intracellular Ca^{2+}increase. *Biochim. Biophys. Acta Mol. Cell Res.* **1999**, *1452*, 151–160. [CrossRef]
45. Salminen,A.;Kaarniranta,K.;Kauppinen,A. CrosstalkbetweenoxidativestressandSIRT 1: Impactontheagingprocess. *Int.J. Mol.Sci.***2013**,*14*,3834–3859.[CrossRef][PubMed]
46. Brand-Williams,W.;Cuvelier,M.E.;Berset,C.Useofaf reeradicalmethodtoevaluateantioxidantactivity .*LWTFoodSci.Technol.* **1995**,*28*,25–30.[CrossRef]
47. Arnao,M.B.;Cano,A.;Hernández-Ruiz,J.;García-Cánovas,F.;Acosta,M.InhibitionbyL-ascorbicacidandotherantioxidantsof the2.2'-azino-bis(3-ethylbenzthiazoline-6-sulfonicacid)oxidationcatalyzedbyperoxidase: Anewapproachfordetermining totalantioxidantstatusoffoods.*Anal.Biochem.***1996**,*236*,255–261.[CrossRef][PubMed]
48. Bochevarov, A.D.; Harder, E.; Hughes, T.F.; Greenwood, J.R.; Braden, D.A.; Philipp, D.M.; Rinaldo, D.; Halls, M.D.; Zhang, J.; Friesner, R.A. Jaguar:A high-performance quantum chemistry software program with strengths in life and materials sciences.*Int. J.QuantumChem.***2013**,*113*,2110–2142.[CrossRef]
49. Spiegel, M.; Gamian, A.; Sroka, Z. A statistically supported antioxidant activity dft benchmark-the effects of hartree-fock exchangeand basis set selection on accuracy and resources uptake. *Molecules* **2021**, *26*, 5058. [CrossRef]
50. Mosmann, T. Rapid colorimetric assay for cellular growth and survival: Application to proliferation and cytotoxicity assays. *J. Immunol. Methods* **1983**, *65*, 55–63. [CrossRef]